ASYMPTOTICS IN SOIL-WHEEL INTERACTION

J.P. Hambleton & A. Drescher
Department of Civil Engineering, University of Minnesota, Minneapolis, MN, USA

ABSTRACT: *Three-dimensional numerical simulations were performed to investigate the asymptotic behavior associated with wide and narrow wheels indenting cohesive and frictional materials. The wheel is taken to be rigid, and the material is elastic-perfectly plastic. Simulations reveal that deformation induced by both wide and narrow wheels can be approximated by plain strain, with the wheel indentation process resembling indentation of a flat punch in both cases. Numerical results are supplemented with a simple, albeit approximate analytic approach that captures essential features of the wheel indentation process and derives from fundamental solutions to the punch problem. Localization present for wide and narrow wheels on frictional soil is attributed to the planar modes of deformation present, as localized deformation was not observed for wheels of intermediate width. Previous studies on soil-wheel interaction assume that deformation occurs only within the plane of the wheel diameter, and the results obtained in this paper point to basic discrepancies arising with this assumption for a narrow wheel, both in terms of the dimensionless force-penetration relationship and soil kinematics.*

1 INTRODUCTION

Wheels of off-road equipment such as hauling trucks, recreational vehicles, and planetary rovers routinely induce permanent deformation in soil. Predicting this deformation, as well as the reaction forces on the wheel, is the central part of many engineering applications, including environmental impact estimation (cf. Li et al., 2007), vehicle mobility assessment (cf. Bekker, 1969; Wong, 2001), and novel methods for characterizing *in situ* material properties over large areas (Hambleton, 2006; Hambleton & Drescher, 2007).

Most approaches for predicting variables of interest in soil-wheel interaction consider deformation only within the diametral plane, i.e., the plane of wheel motion. This assumption is either tacitly or explicitly assumed in empirical methods (Bekker, 1969; Jones et al., 2005), analytic solutions (Karafiath & Nowatzki, 1978; Tordesillas & Shi, 2000), and numerical approaches (Liu and Wong, 1996; Asaf et al., 2006). Theoretical models considering fully three-dimensional soil-wheel interaction have only recently been proposed for cohesive (Hambleton, 2006) and cohesive-frictional soils (Chiroux et al., 2005; Hambleton & Drescher, 2009).

In this paper, the three-dimensional numerical models proposed previously by the authors for indentation of a rigid wheel on cohesive-frictional soil (Hambleton & Drescher, 2009) are used to analyze the asymptotic behavior associated with the width-to-diameter ratio of the wheel going to infinity (wide wheel) and zero (narrow wheel). It is shown that both wide and

narrow wheels are amenable to two-dimensional (plane strain) analysis. An approximate analytic approach is developed based on the numerical results, and appropriate similarity variables for the asymptotic cases are ascertained. Preliminary results from modeling the rolling phase (Hambleton, 2006; Hambleton & Drescher, 2007) suggest that rolling and indentation bear considerable similarity, although the rolling process itself is not considered in this paper.

Due to its relevance in practical applications, focus is directed at the relationship between force and penetration for different wheel geometries and soil properties, although the analysis also provides insight into soil kinematics involved in the indentation process.

2 NUMERICAL SIMULATION

Numerical simulations were performed as described by Hambleton & Drescher (2009). The finite element code ABAQUS/Explicit was used to simulate quasi-static three-dimensional indentation, using the two planes of symmetry involved in wheel indentation to reduce the problem size by a factor of 4. The soil was cohesive-frictional with linear elasticity and perfect plasticity. Plasticity was prescribed according to a modified version of the Drucker-Prager yield condition that closely matches the Mohr-Coulomb condition along compression and extension meridians in principal stress space. Plastic flow was, in general, non-associated. In total, 5 parameters describe the material: Young's modulus E, Poisson's ratio ν, cohesion c, friction angle φ, and dilation angle $\psi \leq \varphi$, where plastic parameters refer to the Mohr-Coulomb yield functions. The wheel was taken to be a rigid cylinder of diameter d and width b.

The soil was modeled as a finite domain of sufficient size such that boundary conditions did not influence results near the wheel. The soil was discretized using roughly 50,000 reduced integration hexahedral elements with linear interpolation, with element length near the wheel being roughly $0.05b$. The wheel was modeled as an analytical (non-discretized) rigid surface with a small edge fillet (radius $0.05b$) to prevent numerical difficulties associated with a sharp edge. Dry friction with coefficient of friction μ was prescribed as the contact law between the soil and wheel, with contact enforced according to the kinematic contact algorithm available in ABAQUS/Explicit.

Numerical simulation consisted of two stages. In the first stage, unit weight γ was applied to the soil in the form of a uniform body force, and in the second stage, the wheel was displaced normally into the soil. Wheel penetration and total force on the wheel are denoted δ and W, respectively. In selected simulations, arbitrary Lagrangian-Eulerian (ALE) adaptivity was used to correct element distortions.

Accuracy of the numerical results is affected by a number of parameters, including element size, time step in the explicit time integration scheme, remeshing increment, and overall duration of simulation (to achieve quasi-static condition). These parameters were chosen based on a previous study in which adequate accuracy was demonstrated for cohesive material (Hambleton, 2006). For the frictional materials addressed in this paper, results were found to be more sensitive to element size than with cohesive material, with wheel force decreasing somewhat at given penetration as element size was decreased. Since the purpose of this paper is to compare results for varying wheel widths, absolute accuracy was not of particular interest. Rather, relative accuracy between simulations of varying wheel width was ensured by keeping the number of elements constant across the wheel width.

3 DIMENSIONAL ANALYSIS

A total of 11 variables appear in the theoretical model described in this paper (W, δ, b, d, c, φ, ψ, γ, E, ν, and μ). Out of several possible choices for dimensionless variables, those that are used in presenting and discussing results are

$$\bar{W} = \frac{W}{\gamma b d^2}, \quad \bar{\delta} = \frac{\delta}{d}, \quad \bar{b} = \frac{b}{d}, \quad \bar{c} = \frac{c}{\gamma d}, \quad \bar{E} = \frac{E}{\gamma d} \tag{1}$$

It should be noted that $\bar{W}$ represents force per unit wheel width. With this, $\bar{W}$ must be independent of wheel aspect ratio $\bar{b}$ for effects out of the diametral plane to be negligible, as assumed in previous works in the literature.

Further simplification is made by limiting attention to specific values of $\bar{E}$, ν, and μ. The case $\bar{E} = 0$ corresponds to a purely elastic material, and $\bar{E} = \infty$ represents rigid-plastic material. The results of simulation presented in this paper are with $\bar{E} = 1000$, which characterizes many geomaterials but also essentially replicates rigid-plastic behavior with all but very small wheel penetration. The overall results are not sensitive to the choice of ν and μ (Hambleton & Drescher 2009), and they were taken as $\nu = 0.3$ and $\mu = 0.5$ in the simulations.

4 NUMERICAL RESULTS

The relationship between $\bar{W}$ and $\bar{\delta}$ for a purely cohesive soil ($\varphi = \psi = 0$) and varying $\bar{b}$ is shown in Fig. 1. As with remaining plots, the discrete data from numerical simulation are plotted as connected points. In this figure, curves from a previous study (Hambleton & Drescher 2009) are supplemented with results for a very narrow wheel. The curve for $\bar{b} = \infty$, corresponding to an infinitely long cylinder, was obtained from a simulation assuming plain strain, taking the same mesh as in the diametral plane of the three-dimensional simulations but with quadrilateral elements. The curves in Fig. 1 are non-smooth as a result of minor discretization error, with nodes at the soil surface coming into contact with the wheel at intervals. The curve for $\bar{b} = 0.02$ is somewhat erratic as a result of remeshing, which was not needed in simulations of other aspect ratios. The need for remeshing points the general difficulty in performing three-dimensional simulations of very narrow wheels. For narrow wheels, element distortion tends to be rather extreme, since element size decreases with the

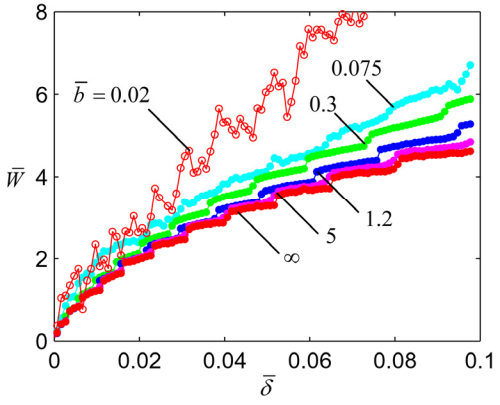

Figure 1. Force-penetration relationship for cohesive soil ($\bar{c}$ = 1.25, $\varphi = 0$) with varying wheel aspect ratio.

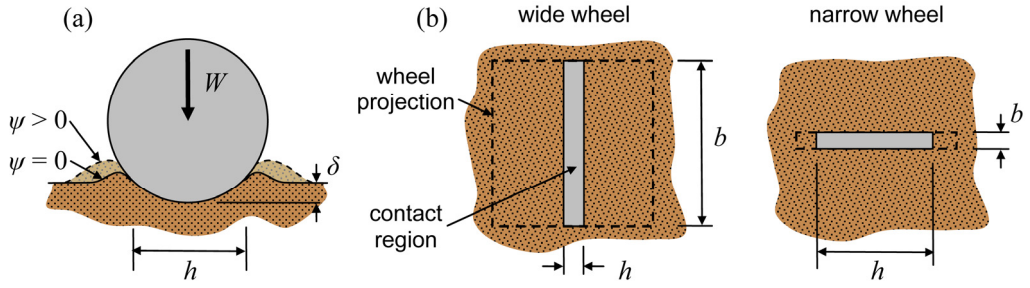

Figure 2. (a) Schematic of wheel indentation and (b) contact area for wide and narrow wheel

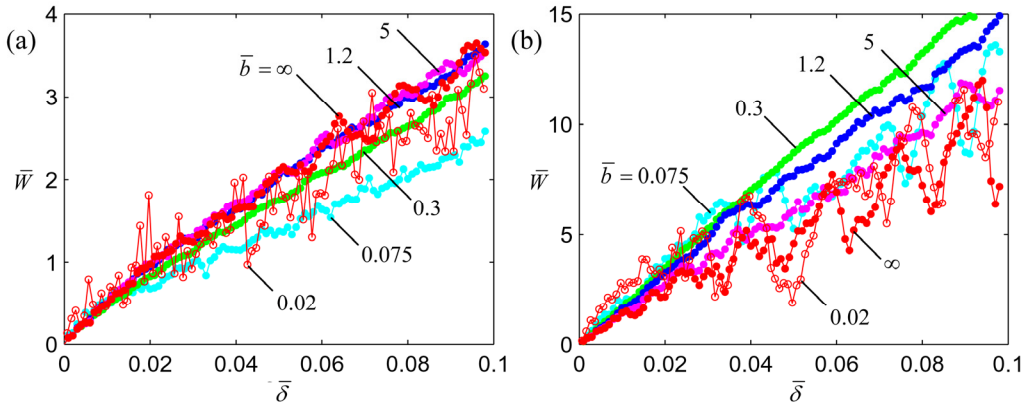

Figure 3. Force-penetration relationship for frictional soil ($\psi = 0$, $\bar{c} = 1.25\times10^{-2}$) with varying wheel aspect ratio: (a) $\varphi = 30°$; (b) $\varphi = 45°$

wheel width but wheel penetration with respect to the diameter remains the relatively small ($\bar{\delta} \le 0.1$). Also, the aspect ratio of elements near the wheel tends to deteriorate as the wheel becomes narrow, as a fine mesh is needed along the wheel width but not in the diametral plane.

For cohesive soil with intermediate and large wheel aspect ratios ($\bar{b} \ge 0.3$), $\bar{b}$ has little influence on $\bar{W}$ at given $\bar{\delta}$, but it is clear that $\bar{W}$ tends to increase as the wheel becomes narrower. In fact, it appears, for fixed $\bar{\delta}$, that $\bar{W}$ becomes unbounded as $\bar{b} \to 0$. As $\bar{b}$ increases, $\bar{W}$ converges to the value obtained assuming plain strain ($\bar{b} = \infty$).

For frictional soil, results from a previous study (Hambleton & Drescher 2009) showed that indentation force depends strongly on dilation angle ψ for wheels with intermediate aspect ratios. The increase in force resulting from an increase in ψ is a consequence of displaced material coming into contact with the wheel in the diametral plane (Fig. 2a). Due to dilation, the amount of material displaced becomes extremely large as ψ approaches φ. To avoid unrealistic deformation, $\psi = 0$ was used in most simulations. Indentation experiments involving granular material also reveal that $\psi = 0$ is reasonable (Drescher et al., 1967).

In Fig. 3, the force-penetration relationship is plotted for varying $\bar{b}$ and two particular values of φ. Very small cohesion was used in the simulations to maintain numerical stability, but the material is purely frictional for practical purposes. Again, remeshing in the simulation with $\bar{b} = 0.02$ causes the curve to look more erratic than with other values of $\bar{b}$. As with cohesive soil, $\bar{W}$ varies significantly as a function of $\bar{b}$. With $\varphi = 30°$ and fixed $\bar{\delta}$, $\bar{W}$ first decreases and then increases as $\bar{b}$ goes from ∞ to 0. The trend is opposite with $\varphi = 45°$, with

$\overline{W}$ increasing and then decreasing as a function of $\overline{b}$. As $\overline{b} \to \infty$ and $\overline{b} \to 0$, fairly regular oscillations (not associated with remeshing) become evident in the force-penetration curves.

In the next section, basic commonalties and differences between the cases $\overline{b} \to \infty$ and $\overline{b} \to 0$ are explained, as well as the trends with respect to $\overline{b}$ noticeable in Figs. 1 and 3.

5 ANALYSIS AND DISCUSSION

Dependence of the force-penetration relationship on wheel aspect ratio $\overline{b}$ rests fundamentally on the evolution of the contact area during indentation. The contact length *h* in the diametral plane (Fig. 2a) grows with increasing penetration in a fairly predictable way. This is shown in Fig. 4 for cohesive and frictional soils, where normalized contact length $\overline{h}$ is very close to the theoretical value obtained by intersecting the undisturbed soil surface with the wheel:

$$\overline{h} = \frac{h}{d} = \sqrt{\overline{\delta} - \overline{\delta}^2} \tag{2}$$

Depending on the aspect ratio and material properties, displaced material moves towards or away from the surface of the wheel, such that contact length deviates somewhat from the value predicted by Eq. (2).

Additional insight into the indentation problem comes from looking at the evolution of average vertical stress *w* acting over the contact area with increasing penetration. Since contact length along the width is fixed at *b* for all values of penetration, *w* is defined as $w = W/(hb)$. Fig. 5 shows normalized average stress, $\overline{w} = w/\gamma d$, evaluated from numerical simulations with cohesive and frictional soils at selected values of penetration (plotted as connected points). With very small penetration, discretization error causes the computed values of *w* to be unreliable, and these points are omitted from the figure.

For cohesive soil, it is seen that $\overline{w}$ increases with increasing $\overline{b}$, with $\overline{w}$ being very close to $(2 + \pi)\overline{c}$ for $\overline{b} = \infty$, corresponding to the theoretical value obtained by Prandtl (1921) for a uniform load on a rigid-perfectly plastic surface (i.e., a flat punch). For $\overline{b} = \infty$, $\overline{w}$ remains virtually constant as a function of $\overline{\delta}$, whereas $\overline{w}$ increases somewhat with $\overline{\delta}$ for relatively narrow wheels. For frictional soil, $\overline{w}$ does not grow monotonically with $\overline{b}$. With relatively small $\overline{\delta}$, $\overline{w}$ is smallest for an intermediate wheel aspect ratio and largest for a very wide wheel ($\overline{b} = \infty$). With relatively large $\overline{\delta}$, $\overline{b} = 0.075$ gives lowest $\overline{w}$, but largest $\overline{w}$ is still associated with the wide wheel. Unlike the behavior observed for cohesive soil, $\overline{w}$ increases as a function of $\overline{\delta}$ for all values of $\overline{b}$, particularly for $\overline{b} = \infty$.

The variations in $\overline{w}$ with $\overline{b}$ shown in Fig. 5 can be linked in part to the ratio *h*/*b*. Irrespective of $\overline{b}$, *h* is greater than *b* when the penetration is very small. For a wide wheel, *h* remains much smaller than *b* (Fig. 2b) for all values of penetration. For a narrow wheel, there is a small value of penetration at which $h = b$, and with further penetration, *h* becomes much larger than *b* (Fig. 2b). When *h*/*b* becomes close to unity, one expects that three-dimensional effects may be significant. When *h*/*b* becomes close to 0, corresponding to a wide wheel ($\overline{b} \to \infty$), the configuration is clearly amenable to plain strain analysis, as illustrated by the agreement between Prandtl's (1921) plain strain punch solution and the numerical results for $\overline{b} = \infty$. With $h/b \to \infty$, corresponding to a very narrow wheel ($\overline{b} \to 0$), it is also reasonable to expect the existence of a state close to plane strain.

For $\overline{b} = 0$, plane strain prevails in the plane associated with the width of the wheel. Viewed in this plane, the problem resembles deep penetration of a flat punch. The width of

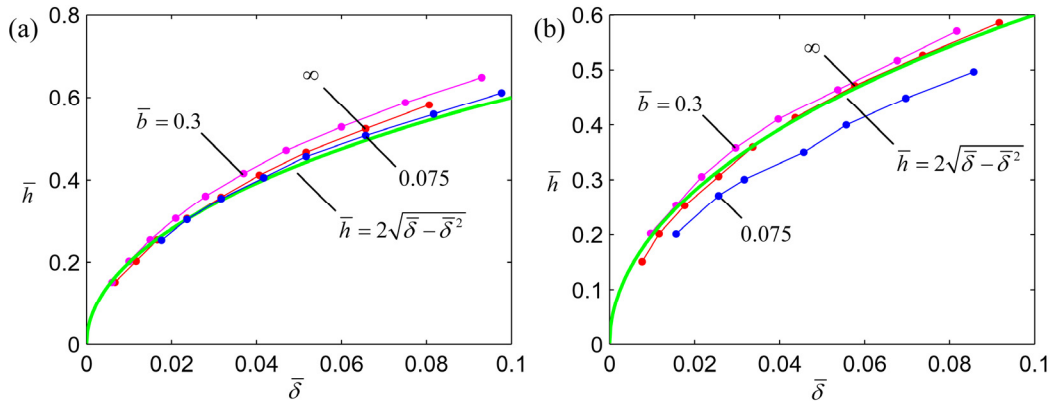

Figure 4. Contact length *vs* penetration for (a) cohesive soil ($\bar{c}$ = 1.25, $\varphi = 0$) and (b) frictional soil ($\varphi = 30°$, $\psi = 0$, $\bar{c}$ = 1.25×10^{-2}).

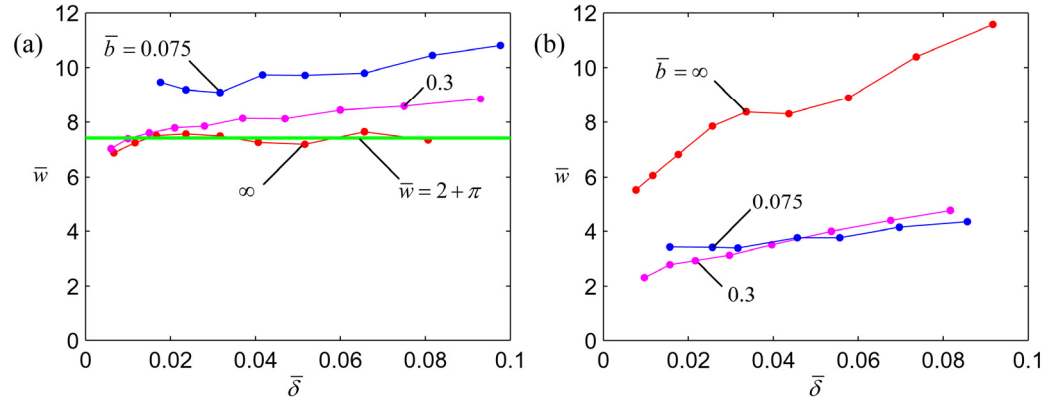

Figure 5. Average stress *vs* penetration for (a) cohesive soil ($\bar{c}$ = 1.25, $\varphi = 0$) and (b) frictional soil ($\varphi = 30°$, $\psi = 0$, $\bar{c}$ = 1.25×10^{-2}).

the punch, denoted b^p, is associated with the width b of a narrow wheel. Fig. 6a shows normalized average stress $w^* = w/b^p$ versus normalized penetration $\delta^* = \delta/b^p$ from a simulation of punch indentation on cohesive soil, where plane strain is assumed and the mesh is comparable to the one used in the plane of the wheel width in three-dimensional simulations. Fig. 6b compares the force-penetration relationship from a simulation with $\bar{b} = 0.04$ to the one obtained through proper scaling of the two-dimensional results: $\bar{W} = \bar{b}\bar{h}w^*$. In the prediction shown in Fig. 7b, Eq. (2) was used together with the equation of regression for w^* (see Fig. 6a). The two-dimensional results match the three-dimensional results well, with small deviation at large $\bar{\delta}$ owing to the increasing significance of three-dimensional effects with increasing $\bar{\delta}$.

The process of a flat punch penetrating soil under plain strain conditions is much better understood that the problem of wheel indentation. In view of the correspondence between the plane strain solution and the behavior with $\bar{b} \to \infty$ and $\bar{b} \to 0$, a simple and approximate analytic approach can be formulated. In this approach, indentation of a wheel is considered as a sequence of limit states corresponding to the punch solution. A somewhat more complicated version of this method including three-dimensional effects was found to provide a satisfactory match to numerical results for wheels with intermediate aspect ratios (Hambleton 2006; Hambleton and Drescher, 2009).

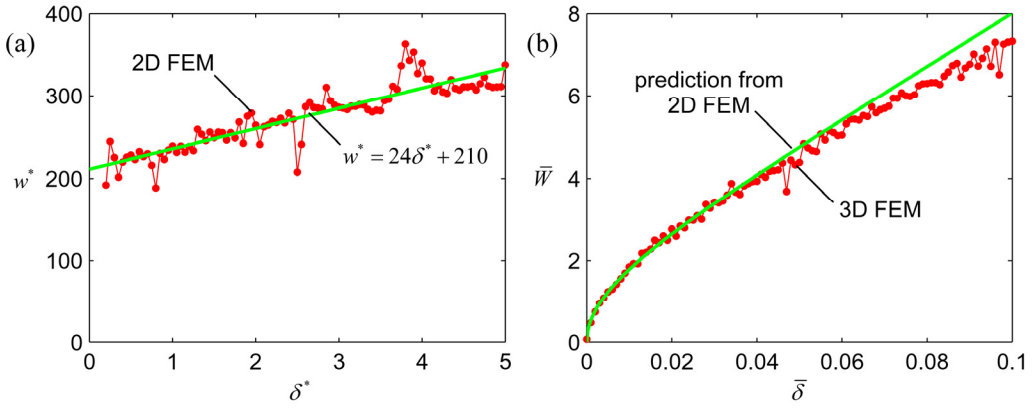

Figure 6. (a) Average stress *vs* penetration for flat punch and plain strain (2D FEM, $c^* = 31$); (b) comparison between plane strain and three-dimensional (3D FEM) predictions of force-penetration curve ($\varphi = 0$, $b/d = 0.04$).

The approach utilizes concepts involved in calculating limit loads on foundations, where average stress on the foundation is calculated as a superposition of effects from cohesion, surcharge, and soil unit weight (Terzaghi, 1943) and so-called "depth factors" are introduced to compensative for the effects of foundation embedment (Meyerhof, 1963). Albeit approximate, the Terzaghi-Meyerhof formula captures the essential features of the punch problem. The formula can be generally expressed as

$$w^* = c^* F_1\left(\varphi, \delta^*\right) + \delta^* F_2\left(\varphi, \delta^*\right) + F_3\left(\varphi, \delta^*\right) \tag{3}$$

Proposed forms for functions F_1, F_2, and F_3 appearing in Eq. (3) can be found in the literature (cf. Das, 2005), with $F_1, F_2, F_3 \geq 0$ for all φ and $F_3 = 0$ for $\varphi = 0$. Dilation angle ψ does not explicitly appear in Eq. (3), as the formula derives from static considerations independent of the flow rule. Theory of rigid, perfectly plasticity is the basis for Eq. (3), such that no elastic parameters are present. Also, the effects of friction along the sides of the punch are not explicitly included in the formulation, although it is expected that increased resistance can be accommodated through the factors F_1, F_2, and F_3. It may be noted that the results shown in Fig. 6a for $\varphi = 0$ are consistent with the approximation in Eq. (3), with F_1 and F_2 simply being constants and $F_3 = 0$.

In the next sections, Eq. (3) is used as the basis for approximating the asymptotic behavior associated with $\bar{b} = \infty$ and $\bar{b} = 0$ for cohesive ($\varphi = 0$) and frictional ($\bar{c} = 0$) soils. In all cases, total force $\bar{W}$ is computed as a product of average stress $\bar{w}$ and contact area, where

$$\bar{W} = \bar{w}\bar{h} \tag{4}$$

The punch variables and the wheel variables are related through

$$\bar{\delta} = \frac{b^p}{d}\delta^*, \quad \bar{w} = \frac{b^p}{d}w^*, \quad \bar{c} = \frac{b^p}{d}c^* \tag{5}$$

For a wide wheel, $b^p = h$ and δ^* is effectively zero, as the equivalent flat punch replacing the wheel remains at the surface but grows in width as a function of penetration. For a narrow wheel, $b^p = b$ and $\delta^* > 0$.

5.1 Wide wheel on cohesive soil

For a wide wheel ($\bar{b} = \infty$) on cohesive soil ($\varphi = 0$), $\bar{W}$ is given by

$$\bar{W} = 2\sqrt{\bar{\delta} - \bar{\delta}^2}\,\bar{c}F_1 \tag{6}$$

where $F_1 \approx 2 + \pi$ (see numerical results in Fig. 6a). Eq. (6) was obtained by combining Eqs. (2)-(5), as well as considering $b^p = h$ and $\delta^* = 0$. In this case, vertical force simply scales with cohesion, and unit weight does not play a role.

5.2 Narrow wheel on cohesive soil

Normalized force for a narrow wheel ($\bar{b} = 0$) on cohesive soil ($\varphi = 0$) takes the form

$$\bar{W} = 2\sqrt{\bar{\delta} - \bar{\delta}^2}\left[\bar{c}F_1 + \bar{\delta}F_2\right] \tag{7}$$

where F_1 and F_2 are functions of $\delta^* = \bar{\delta}/\bar{b}$ only. Compared to the case $\bar{b} = \infty$ (Eq. (6)), there is an extra term in Eq. (7) and the function F_1 also includes the effects of δ^*. Since $\delta^* \to \infty$ as $\bar{b} \to 0$, functions F_1 and F_2 can be quite large for a narrow wheel. Overall, Eq. (7) reveals that $\bar{W}$ should increase as $\bar{b}$ decreases, which is the behavior determined from numerical simulation (Fig. 1).

5.3 Wide wheel on frictional soil

For a wide wheel ($\bar{b} = \infty$) on frictional soil ($\bar{c} = 0$), one finds

$$\bar{W} = 2\sqrt{\bar{\delta} - \bar{\delta}^2}\left[\bar{\delta}F_2 + 2\sqrt{\bar{\delta} - \bar{\delta}^2}F_3\right] \tag{8}$$

where F_2 and F_3 are functions of φ only ($\delta^* = 0$). An important feature of Eq. (8) is the second term in the brackets, which depends on $\bar{\delta}$ as a consequence of $b^p = h$. The term in brackets is in fact $\bar{w}$, and the relatively strong dependence of $\bar{w}$ on $\bar{\delta}$ is corroborated by the trend in numerical results shown in Fig. 5b for $\bar{b} = \infty$.

5.4 Narrow wheel on frictional soil

The force-penetration relationship for a narrow wheel ($\bar{b} \to 0$) on frictional soil ($\bar{c} = 0$) is

$$\bar{W} = 2\sqrt{\bar{\delta} - \bar{\delta}^2}\left[\bar{\delta}F_2 + \bar{b}F_3\right] \tag{9}$$

where F_2 is a function of both φ and δ^*. In contrast to $\bar{b} = \infty$ (Eq. (8)), the factor in front of F_3 does not depend on $\bar{\delta}$. This implies that averages stress, given in square brackets in Eq. (9), should not increase as rapidly with penetration as with $\bar{b} = \infty$. Again, numerical results support this conclusion (Fig. 5b). However, there are also competing factors in the term involving F_3, since F_3 depends on δ^* and $\delta^* = \bar{\delta}/\bar{b} \to \infty$ as $\bar{b} \to 0$. If F_3 is linear or lower order in δ^*, this term will vanish as $\bar{b} \to 0$.

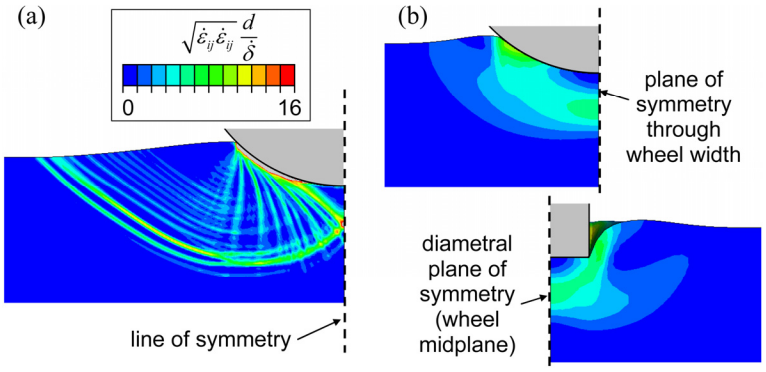

Figure 7. Deviatoric strain rate from (a) plane strain and (b) three-dimensional simulations ($\bar{b}$ = 0.3) with frictional soil ($\varphi = 15°$, $\psi = 0$, $\bar{c}$ = 1.25×10^{-2})

6 LOCALIZATION

The regular oscillations in $\bar{W}$ distinguishable for $\bar{b} = \infty$ in Fig. 2 can be attributed to the presence of localized deformation. Fig. 7 shows deviatoric strain rate in the soil for $\bar{b} = \infty$, where strain rate is normalized by d and the penetration velocity of the wheel $\dot{\delta}$ (see legend in Fig. 7). Also shown for comparison are results from a three-dimensional simulation with $\bar{b} = 0.3$, where strain rate is plotted along the two planes of symmetry. Localized deformation is evident for $\bar{b} = \infty$ but does not appear with $\bar{b} = 0.3$. The oscillations in force for narrow wheels (Fig. 2) can likewise be ascribed to localization, as this effect is known to occur in the analogous punch indentation problem.

The presence of strain localization for $\bar{b} \to \infty$ and $\bar{b} \to 0$ appears to be closely related to the planar modes of deformation occurring in these cases. For intermediate geometries (e.g., $\bar{b}$ = 0.3), localization is suppressed as a result of inherently three-dimensional (non-planar) deformation. It is known, for instance, that strong discontinuities in incremental material displacement are inhibited in axisymmetry (Cox et al., 1961).

7 CONCLUDING REMARKS

Three-dimensional numerical simulations of rigid wheels of varying width indenting cohesive and frictional materials reveal that plane strain prevails with both $\bar{b} \to \infty$ (wide wheels) and $\bar{b} \to 0$ (narrow wheels). For wide wheels, indentation bears considerable similarity to shallow indentation of a flat punch, with a growing contact region in the diametral plane. For narrow wheels, indentation can be likened to deep indentation of a flat punch where contact length does not grow in the plane of dominant deformation but penetration is large with respect to width of the wheel, such that effects like material weight and sidewall friction become important. Since displaced material does not contribute to an increase in contact area for a very thin wheel, dilation angle can be expected to effect wheel force less than for wheels with intermediate or large width. Numerical simulations also reveal the presence of localized deformation for wide and narrow wheels on frictional soil, whereas non-planar deformation for wheels of intermediate aspect ratio tends to suppress localization.

Previous studies in soil-wheel interaction largely assumed that deformation occurs only within the diametral plane. This assumption, while valid for a wide wheel, disregards basic factors governing the force-penetration relationship for narrow wheels, as well as essential kinematical features of the problem. For a narrow wheel, deformation is almost exclusively within the plane of the wheel width, and errors in the force-penetration relationship predicted

by disregarding effects in this plane depends on the wheel geometry and material properties, being large in some cases and small for others. The approximate analytic method presented in this paper captures the influence of parameters on the force-penetration relationship for wide and narrow wheels in a tractable way.

ACKNOWLEDGEMENTS

Financial support for this research was provided by the Shimizu Corporation. Computer resources from the Minnesota Supercomputing Institute are also gratefully acknowledged.

REFERENCES

Asaf, Z., Shmulevich, I. & Rubinstein, D. (2006), "Predicting soil-rigid wheel performance using distinct element methods". Trans. ASABE, Vol. 49(3), 607-616.

Bekker, M.G. (1969), Introduction to Terrain-Vehicle Systems, University of Michigan Press, Ann Harbor, MI.

Chiroux, R.C., Foster Jr., W.A., Johnson, C.E., Shoop, S.A. & Raper, R.L. (2005), "Three-dimensional finite element analysis of soil interaction with a rigid wheel". Appl. Math. Comp., Vol. 162(2), 707-722.

Cox, A.D., Eason, G. & Hopkins, H.G. (1961), "Axially symmetric plastic deformation in soils". Phil. Trans. Roy. Soc. A, Vol. 254(1036), 1-45.

Das, B.M. (2005), Fundamentals of Geotechnical Engineering, Thomson, Toronto, ON.

Drescher A, Kwaszczynska K, Mroz Z. (1967), "Static and kinematics of the granular medium in the case of wedge indentation". Arch. Mech. Stos., Vol. 19, 99-113.

Hambleton, J.P. (2006), Modeling Test Rolling in Clay, MS Thesis, University of Minnesota, Minneapolis, MN.

Hambleton, J.P. and Drescher, A. (2008), "Soil damage models for off-road vehicles", Proceedings of GeoCongress 2008, Geosustainability and Geohazard Mitigation, New Orleans, USA, p. 562-569.

Hambleton, J.P. Drescher A. (2007), "Modeling test rolling on cohesive subgrades", Proceedings of the International Conference on Advanced Characterisation of Pavement and Soil Engineering Materials, Athens, Greece, p. 359-368.

Hambleton, J.P. & Drescher, A. (2009), "Modeling wheel-induced rutting in soils: Indentation". J. Terramech., in press.

Jones, R., Horner, D., Sullivan, P. & Ahlvin, R. (2005), "A methodology for quantitatively assessing vehicular rutting on terrains". J. Terramech., Vol. 42(3-4), 245-257.

Karafiath, L.L. & Nowatzki, E.A. (1978), Soil Mechanics for Off-Road Vehicle Engineering, Trans Tech Publications, Clausthal.

Li, Q., Ayers, P.D. & Anderson, A.B. (2007), "Prediction of impacts of wheeled vehicles on terrain." J. Terramech., Vol. 44(2), 205-215.

Liu, C.H. & Wong, J.Y. (1996), "Numerical simulations of tire-soil interaction based on critical state soil mechanics". J. Terramech., Vol. 33(5), 209-221.

Meyerhof, G.G. (1963), "Some recent research on bearing capacity of foundations." Can. Geotechnical J., Vol. 1(1), 16-26.

Prandtl, L. (1921), "Über die Eindringungsfestigkeit (Härte) plastischer Baustoffe und die Festigkeit von Schneiden." Zeit. fur angewandte Mathematik Mechanik, Vol. 1(1), 15-20.

Terzaghi, K. (1943), Theoretical Soil Mechanics, Wiley, New York, NY.

Tordesillas, A. & Shi, J. (2000), "Frictionless rolling contact of a rigid circular cylinder on a semi-infinite granular material". J. Eng. Math., Vol. 37(1-3), 231-252.

Wong J.Y. (2001), Theory of Ground Vehicles, Wiley, New York, NY.